ORIGINAL ARTICLE

lajss.org
Latin American Journal of Solids and Structures

www.lajss.org

Experimental research on dynamic mechanical characteristics of layered composite coal-rock

Shizhuo Zou[a], Li Wang[b], Jianmin Wen[a], Xiaoling Wu[a], Yu Zhou[a*]

[a]Key Laboratory of Ministry for Efficient Mining and Safety of Metal Mines, University of Science and Technology Beijing, Beijing 100083, China. E-mail: 2267725130@qq.com, 1147212361@qq.com, 1035777942@qq.com, westboy85@ustb.edu.cn
[b]PowerChina Road Bridge Group Co., Ltd., Beijing 100048, China. E-mail: 752279087@qq.com

* Corresponding author

https://doi.org/10.1590/1679-78256721

Abstract

Using the Separate Hopkinson Pressure Bar test device, a series of dynamic impact tests were carried out on the single coal and white sandstone near the incident bar. When the stress wave propagates in a complex with different wave impedance matching effects, its dynamic mechanical properties change, energy dissipation law and damage characteristics are studied. The research results show that: (1) With the increase of impact velocity, the peak stress and DIF of layered composite coal-rock increase linearly. At the same speed, when the stress wave changes from hard to soft, the peak stress and DIF are larger than the stress wave from soft to hard. (2) The dissipated energy density of layered composite coal-rock increases in a quadratic function with the increase of the incident energy density, and the composite body with better wave impedance matching effect has a higher dissipated energy density. (3) The fractal dimension and the degree of fracture of layered composite coal-rock increase with the increase of the speed. The white sandstone component is mostly shear failure, and the coal component is mostly crushed.

Keywords

layered composite coal-rock; SHPB; wave impedance; fractal; energy dissipation; dynamic mechanical properties

Graphical Abstract

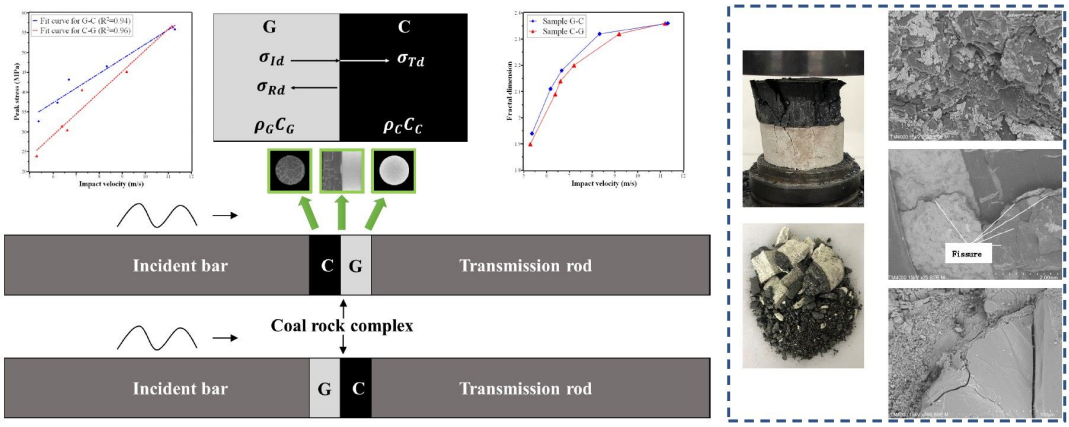

Received September 02, 2021. In revised form October 09, 2021. Accepted October 09, 2021. Available online October 13, 2021
https://doi.org/10.1590/1679-78256721

1 INTRODUCTION

The layered composite coal-rock composed of single coal and rocks of different lithologies superimposed in a certain order is very common in geological construction, mine excavation, and tunnel excavation. The layered composite coal-rock is different from a single rock body and exhibits different properties in the process of energy transfer and attenuation. Due to the complexity of its own structure, the study of its mechanical properties under dynamic impact is of great significance to blasting and development, like in Dou et al. (2006), Zhao et al. (2008), Shan & Lai (2020), Wang et al. (2020) and Shen (2014).

At present, there are many related researches on the static mechanical properties of layered composites. Liu et al. (2018a) used strain gauges to obtain the stress and strain changes in the coal-rock assembly, and established the damage constitutive model of the coal monomer when the coal monomer is connected with one or two rocks in series. Li et al. (2018b) used the relationship between fractal dimension and loading speed value to discuss the failure mechanism of rock under the condition of uniaxial cyclic loading and unloading. Wen et al. (2017) studied the damage stage changes of coal and rock samples under uniaxial compression under the size effect through PFC2D software based on particle flow and acoustic emission (AE) research methods. Huang et al. (2011) modified the original hydraulic fracturing method, and proposed the use of directional fracturing technology after pre-hydraulic fracturing and slotting and hydraulic blasting fracturing weak and strong anti-permeability technology to carry out structural transformation of coal and rock masses. Thereby preventing gas outburst. Guo et al. (2011) conducted tests and numerical simulations to cross-validate the fracture mechanism and strength characteristics of coal-rock assemblies with built-in dip angles, and obtained the macroscopic failure mechanism of coal-rock assemblies with built-in dip angles, and the interface between coal and rock Influence. Zuo et al. (2011) carried out uniaxial and triaxial compression tests on rocks, coal-rock assemblages, and coal, respectively, and analyzed their failure mechanisms and mechanical behaviors under different stress conditions, as well as the similarities and differences between them. Based on elastic mechanics and damage mechanics, Li et al. (2021) established a special elastoplastic catastrophic rockburst model of coal with structural planes, introduced and studied the concept of coal and rock volume energy, and explained the evolution process of rockburst. Song et al. (2012) established the relationship between electromagnetic radiation (EMR) and dissipated energy by studying the energy conversion process in the destruction of coal-rock assembly and using voltage amplitude.

However, in actual situations, research on dynamic mechanical properties will bring greater help to underground construction. The impact dynamic performance change of the layered composite body under dynamic load has great reference significance for underground rock drilling and blasting engineering. Yin et al. (2016) used a split Hopkinson pressure bar device (SHPB) to study the physical and mechanical properties of coal-rock assembly after treatment at different temperatures and found that coal-rock has a significant temperature effect. Chen (2018) used the LS-DYNA module in ANSYS software to establish four rock-coal-rock combinations with different height ratios, and conducted a Hopkinson pressure bar test, and found that the failure of the coal-rock combination is mainly related to coal and rock. Has little relation with impact speed and combination mode. Gong et al. (2018) used the split Hopkinson compression bar test to explore the changes in the mechanical behavior of the coal-rock assembly under the condition of high strain rate, and found that the dynamic compressive strength and peak strain of the coal-rock assembly have obvious Loading rate effect.

At present, scholars have used theoretical analysis, numerical simulation, dynamic impact test and other methods to carry out some researches on the static impact load and the performance change under dynamic impact load of the layered composite coal-rock. There are few reports on the study of dynamic shock in different directions. In this test, the separated Hopkinson pressure bar experimental device (SHPB) is used to carry out impact load test on the layered coal-rock assembly in three speed ranges, and analyze its dynamic mechanical properties and failure mechanism. At the same time, the energy dissipation theory is used to analyze the stress Quantitative analysis of energy changes in the process of blast wave transmission, fractal theory is adopted to study the broken shape of the material, and the dynamic characteristics and failure characteristics of the layered composite coal-rock are revealed. The research results can provide theoretical guidance for rock breaking and blasting in composite rock mass engineering.

2 Experimental design

2.1 Sample preparation of layered composite coal-rock

The sample is a composite of coal monomer and roof rock white sandstone, which is common in coal mines. Both rocks are taken from a mine in Xinxiang, Henan. The white sandstone and coal monomer are hard rock and soft rock, respectively. In order to ensure the consistency of the performance of the rock samples, one-time coring and cutting are performed on the same uniform and complete rock. Under the premise of consistent mechanical properties, they are processed into a cylindrical rock sample of φ50mm×25mm and separately Keep two φ50mm×100mm cylinder standard samples,this process strictly complies with ISRM recommended standards, and use a grinder to polish the two end faces

of the rock sample to control the non-parallelism and non-perpendicularity of the section within ±0.02mm. Compared with coal alone, white sandstone is a harder rock. For composite soft and hard rock masses, studies have shown that brittle materials such as epoxy resin can simulate rock mechanical behavior well, like in Li et al. (2019). Therefore, this experiment uses epoxy resin to complete the splicing of the processed coal monomer and the white sandstone rock sample. The thickness of the epoxy resin is strictly controlled during this process. The finished sample is shown in Figure 1. The sample is divided into two groups according to the direction of shock wave action. They are the white sandstone-coal monomer complex from hard to soft, denoted as GC, and the coal monomer-white sandstone complex from soft to hard, denoted as CG, as shown in Figure 2.

Figure 1 Physical image of the sample

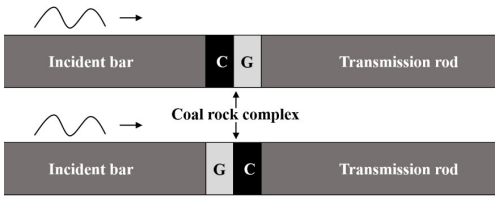

Figure 2 Schematic diagram of sample grouping

Three-dimensional CT scanning was performed on the stitched layered composite coal-rock. The test instrument used the NanoVoxel-3502E high-resolution X-ray three-dimensional tomography imaging system produced by Tianjin Sanying Company, China. The scanning voltage was 160 kV, the current was 45 μA, and the resolution was 37.79. μm, the scanning method is CT spiral scanning, the number of scanning frames is 1440 frames/circle, the exposure time is 0.3 μs, and the number of image merging is 2. The sample microstructure scan is shown in Figure 3.

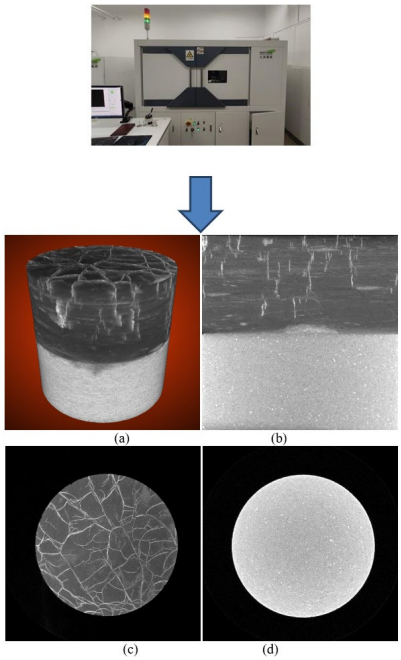

Figure 3 CT scan of the internal structure of layered composite coal-rock. (a) Three-dimensional view of layered composite coal-rock; (b) Longitudinal section view of layered composite coal-rock; (c) Cross-sectional view of single coal; (d) Cross-sectional view of white sandstone

In order to determine the vein-like white thin line components in the coal sample in the CT image, the white sandstone and the single coal sample were taken for EDS (Energy Dispersive Spectroscopy) surface scanning. The scanning results are shown in Figure 4. In Figure 4(a), the main elements in the white sandstone are Si, O, AI, etc., and no abnormal components appear. In Figure 4(b), the main elements of the white thin lines distributed in the shape of veins in the coal monomer are Ca, O, Si, etc. The analyzed components are limestone, quartz, etc., which are trace impurities in the deposition and formation process of the coal monomer. It is a normal phenomenon and will not affect the results of the experiment.

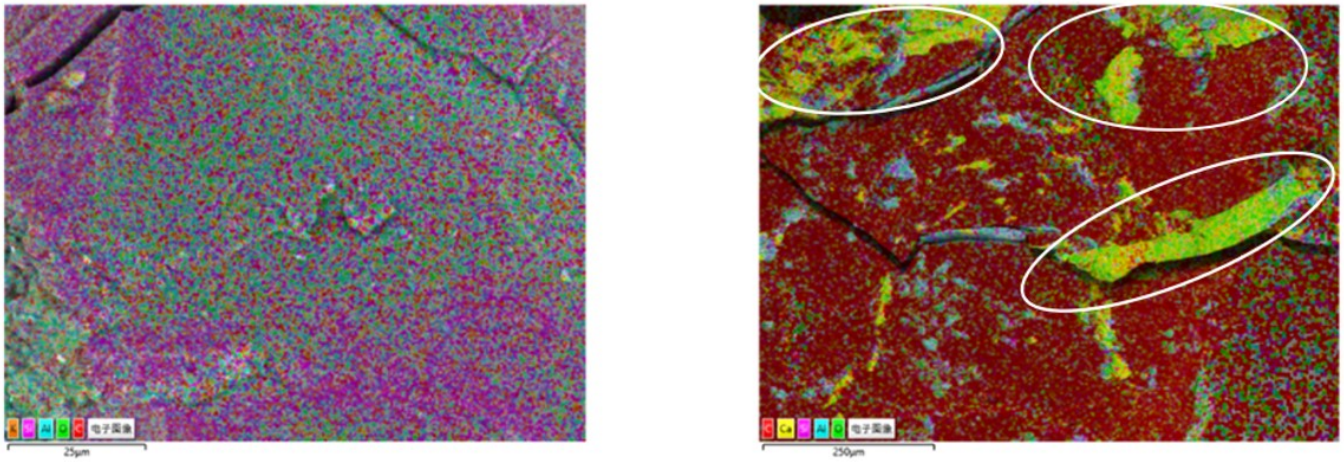

(a) Energy spectrum scan of white sandstone (b) Energy spectrum scan of coal monomer

Figure 4. Scanning diagram of energy dispersive spectrometer

2.2Test device

The instrument used to measure the static mechanical parameters of the standard sample and the layered composite coal-rock is the YAW-600 computer-controlled electro-hydraulic servo rock pressure testing machine. As shown in Figure 5, the testing machine has an electro-hydraulic servo pressure testing machine with force closed-loop control, which has constant stress control and load retention functions. The testing machine is divided into two parts: a loading device and a servo oil source. The loading speed of this experiment is set 100N/s, when the residual stress reaches 60%, stop loading.

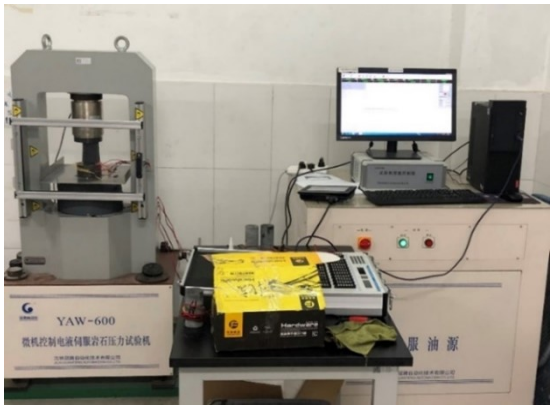

Figure 5. Microcomputer controlled electro-hydraulic servo rock pressure testing machine

In order to study the dynamic mechanical properties of the layered composite coal-rock, this experiment uses the separate Hopkinson pressure bar test device (SHPB) to complete the dynamic impact experiment.The impact speed is mainly controlled by the set air pressure and the depth of the spindle-shaped bullet, and is proportional to the relationship. As shown in Figure 6(a) and 7(b), the diameter of the pressure rod is 50 mm, the bullet is spindle-shaped, the shock wave waveform is sine wave, the incident rod and transmission rod are 2.5 m, the material is alloy steel, and the density is 7.8× 103 kg/m^3, elastic modulus of 240 GPa, longitudinal wave velocity of 5200 m/s. The data acquisition

system consists of Beidaihe SDY2107A super dynamic strain gauge and Yokowaga-DL850E oscilloscope, timing equipment adopts JXCS-02 type chronograph.

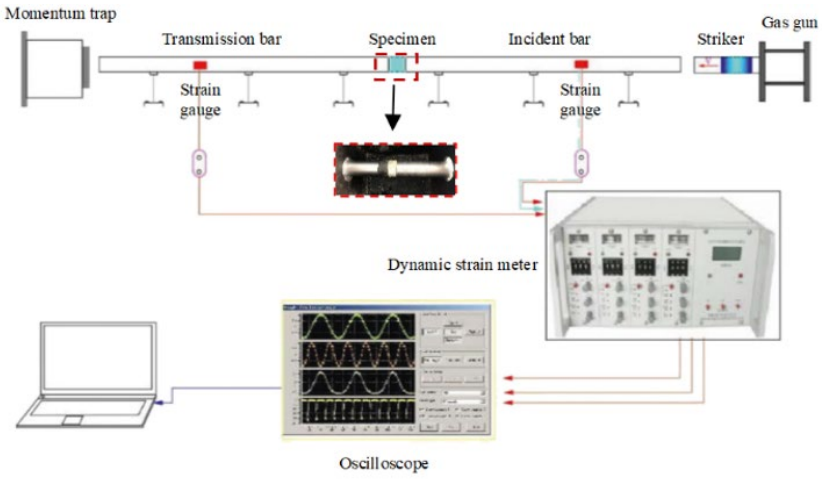

(a) Schematic diagram of SHPB device

(b) Schematic diagram of SHPB device

Figure 6. Microcomputer controlled electro-hydraulic servo rock pressure testing machine

In the test, the incident, reflected and projected signals are collected through the strain gauges on the surface of the strut. The typical waveforms measured in the test are shown in Figure 7.

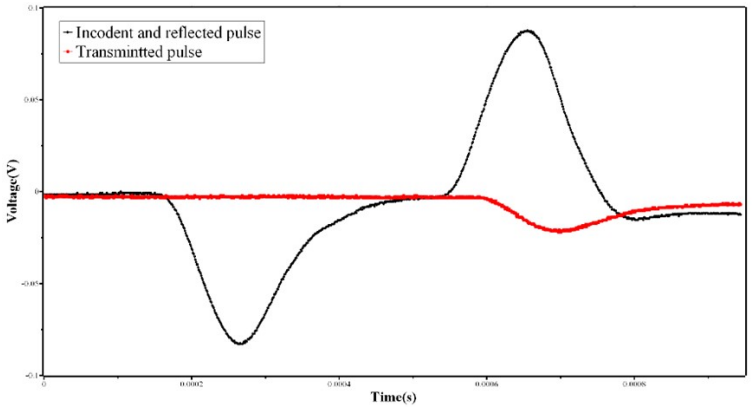

Figure 7. Typical incident, reflection, and transmission waveforms of layered composite coal-rock

2.3Data processing

Affected by the set air pressure and uniaxial impact, the spindle-shaped bullet will initiate an impact on the input rod with the set air pressure. Due to the manual error in the air pressure setting and the systematic error of the warhead position, the speed will have an up and down deviation within the set value range. In this process, according to the one-dimensional stress wave theory, the stress, strain, and strain rate of the specimen satisfy the following relationship,like in Zhao et al. (2019):

$$\sigma(t) = \frac{A_e E_e}{2A_S}[\varepsilon_I(t) + \varepsilon_R(t) + \varepsilon_T(t)] \tag{1}$$

$$\varepsilon(t) = \frac{C_e}{L_s}\int_0^t [\varepsilon_I(t) - \varepsilon_R(t) - \varepsilon_T(t)]\, dt \tag{2}$$

$$\dot{\varepsilon}(t) = \frac{C_e}{L_S}[\varepsilon_I(t) - \varepsilon_R(t) - \varepsilon_T(t)] \tag{3}$$

In the formula,$\varepsilon_I(t)$, $\varepsilon_R(t)$, and $\varepsilon_T(t)$ are the strain generated by the incident wave, reflected wave, and transmitted wave, respectively; A_e andE_e are the elastic modulus and cross-sectional area of the strut; C_e is the stress wave in The propagation velocity in the pressure rod; A_S and L_s are the initial cross-sectional area and initial length of the specimen, respectively.

However, when the traditional three-wave method is used for data processing, the incident signal and the reflected signal collected in the experiment are very close. When calculating the incident end stress, the calculation results are often completely inconsistent due to the error of the test data, like in Zhu (2009) [[Q2: Q2]]. In view of the particularity of the layered composite coal-rock, this test considers the balance of forces at both ends of the specimen, that is:

$$\varepsilon_I(t) + \varepsilon_R(t) = \varepsilon_T(t) \tag{4}$$

Substituting formula (4) into formula (1) to obtain a simplified three-wave calculation formula, that is, the stress, strain, and strain rate are calculated using the following formula:

$$\sigma(t) = \frac{A_e E_e}{A_S}\varepsilon_T(t) \tag{5}$$

$$\varepsilon(t) = \frac{-2C_e}{L_s}\int_0^t \varepsilon_R(t)\, dt \tag{6}$$

$$\dot{\varepsilon}(t) = \frac{-2C_e}{L_S}\varepsilon_R(t) \tag{7}$$

2.4Test plan

There are a total of 4 standard samples for the experimental test of static mechanical parameters of the layered composite coal-rock, and a total of 6 composites. Standard samples are used to measure various parameters of coal monomer and white sandstone, and each sample is tested twice. Divide the composite into two groups according to the direction of shock wave impact of the sample, each group has 3, and the uniaxial compressive strength is measured respectively.

There are a total of 14 composites tested in the dynamic mechanical parameter test of the layered composite coal-rock, which are divided into 2 groups according to the direction of the shock wave acting on the samples, with 7 in each group. A total of three uniaxial impact tests with different speed ranges are set, 5-7m/s is the low-speed range, a total of two samples; 7-9m/s is the medium-speed range, a total of two samples; 9-11m/s is There are two samples in the high-speed zone. Because the SHPB experiment has a strong uncertainty, each group set a layered composite coal-rock as a supplementary sample. The layered composite coal-rock was used as a candidate impact sample. Before the test, a small amount of butter was evenly applied as a lubricant to both ends of the layered composite coal-rock to reduce the effect of section friction. The samples are grouped and numbered according to the impact direction. Taking CG-1 as an example, CG represents the single coal as the rock sample under the shock wave and is close to the incident rod, and 1 is the serial number. The specific parameters of the sample are shown in Table 1.

Table 1. Specific parameters of the layered composite coal-rock sample

Group number	Sample number	Diameter Φ (mm)	Quality m(g)	Apparent density ρ (g/cm^3)	Longitudinal wave velocity V(m/s)	Wave impedance ($g/cm^3 \cdot m/s$)	Design speed V (m/s)
1	CG-1	50.3	198	2.00	2065	4130.00	Low
	CG-2	50.4	198	2.00	2100	4200.00	Low
	CG-3	50.0	189	1.93	1985	3831.05	Medium
	CG-4	50.5	195	1.97	2085	4107.45	Medium
	CG-5	50.0	190	1.94	2190	4248.60	High
	CG-6	50.0	197	2.01	2020	4060.20	High
	CG-7	50.5	190	1.92	2100	4032.00	
2	GC-1	50.0	191	1.95	2045	3987.75	Low
	GC-2	50.5	189	1.91	2215	4230.65	Low
	GC-3	50.9	190	1.90	2220	4218.00	Medium
	GC-4	50.3	195	1.97	1885	3713.45	Medium
	GC-5	50.3	197	1.99	2080	4139.20	High
	GC-6	50.5	198	2.00	2240	4480.00	High
	GC-7	50.2	197	2.00	1945	3890.00	

3 Experimental results

3.1Composite mechanical properties

3.1.1 Static mechanical properties

The wave velocity and uniaxial compressive strength of the standard block were measured by a non-metal ultrasonic detector and a computer-controlled electro-hydraulic servo rock pressure tester. The basic mechanical parameters after measurement are shown in Table 2. It can be seen from the wave impedance and elastic modulus that the strength of white sandstone is higher than that of coal alone, and the composite is a typical soft-hard rock layered composite.And it can be found that the wave impedance of the layered coal-rock complex is approximately equal to half of the sum of the two individual wave impedances.

Table 2 Basic physical and mechanical parameters of rock

Rock types	Density (g/cm^3)	Wave speed (m/s)	Wave impedance ($g/cm^3 \cdot m/s$)	Uniaxial compressive strength (MPa)	Modulus of elasticity (GPa)
Coal monomer	1.46	1797	2623.62	14.33	2.43
White sandstone	2.40	2475	5940.00	45.07	4.20

Figure 8 shows the uniaxial compressive stress-strain curves of layered coal-rock assemblies in different directions. It can be found that the uniaxial compressive strength of layered coal-rock assemblies does not have much relationship with the direction of impact, and the direction of impact will affect the compression period. Strain-strain time history. The C-G combination will reach the compressive strength and break earlier than the G-C combination. During the loading process of the composite body, the composite body continuously accumulates energy. The energy limit of the coal component is smaller than that of the white sandstone. Therefore, when the coal component is close to the compression direction, it will be easier to reach than the white sandstone. Destroyed by the limit of energy storage. The moment the coal component is destroyed, a large amount of elastic energy will be released to the white sandstone, which will eventually lead to the overall rupture of the composite. When the white sandstone is close to the incident direction, the energy will first be absorbed inside the white sandstone and then reach the coal component to incubate the internal fissures. Therefore, the C-G complex will be destroyed earlier than the G-C complex. The compressive strength of the layered coal-rock assembly is also slightly improved compared to the monomer components. It can be found that the increase in the compressive strength of the assembly is related to the softer rock.

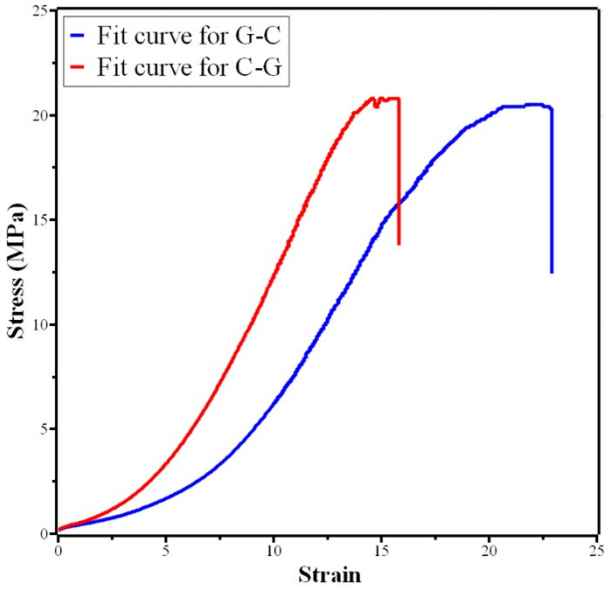

Figure 8: Uniaxial compression stress-strain curve of layered coal and rock assembly

3.1.2 Dynamic mechanical properties

The layered composite coal-rock is a combination of rock and coal with different properties and components, and is more common in coal mines. The attenuation and propagation of stress waves in the layered composite coal-rock will affect the changes in its dynamic mechanical properties, and thus affect various fields such as engineering blasting, geological prospecting, and earthquake protection. In order to compare the strength of the material under impact load and static load and optimize engineering parameters, the dynamic increase factor DIF (Dynamic Increase Factor),like in Malvar and Crawford (1998), Feng et al. (2020) and Comité Euro-International du Béton (1993), which is commonly used in the concrete field, is introduced here, namely

$$DIF = \frac{f_{cd}}{f_{cs}} \tag{8}$$

In the formula, f_{cd} is the dynamic compressive strength of the layered composite coal-rock, and f_{cs} is the static compressive strength of the layered composite coal-rock.

Section 3.1.1 measured the static compressive strength of the layered composite coal-rock as 20.67MPa, and the dynamic compressive strength was measured by the SHPB test. The main dynamic mechanical parameters are shown in Table 3.

Table 3 Main dynamic mechanical parameters of layered composite coal

Sample number	Density ρ(kg/m^3)	Impact velocity (m/s)	Peak stress f_c(MPa)	Peak strain ε(×10^{-3})	Dynamic IncreaseFactor DIF
CG-1	2004.78	5.29	23.94	15.77	1.16
CG-2	2000.80	6.38	31.39	20.88	1.52
CG-3	1925.14	6.61	30.43	16.56	1.47
CG-4	1966.59	7.21	41.41	16.77	2.00
CG-5	1935.32	9.19	45.17	25.08	2.19
CG-6	2006.63	11.20	56.47	27.80	2.73
GC-1	1945.51	5.36	31.90	14.61	1.54
GC-2	1906.08	6.18	37.56	20.63	1.82
GC-3	1901.10	6.66	43.87	19.33	2.12
GC-4	1974.41	8.33	46.20	17.35	2.24
GC-5	1994.66	11.32	55.62	21.78	2.69

3.1.2.1 Dynamic stress-strain relationship

Figure 9 shows the equivalent stress-strain curves of the C-G composite and G-C composite in the low, medium and high impact velocity ranges. During the loading period, the change trend of the layered composite rock mass is basically the same. After a short linear elastic stage, the dynamic stress-strain curve begins to increase first and then decrease. As the impact velocity continues to increase, the CG composite and both the dynamic elastic modulus and peak stress of the GC composite show an increasing trend. When the dynamic load gradually increases, the layered composite body enters the compaction section, and then the sample begins to shape and collapse until it finally fails.

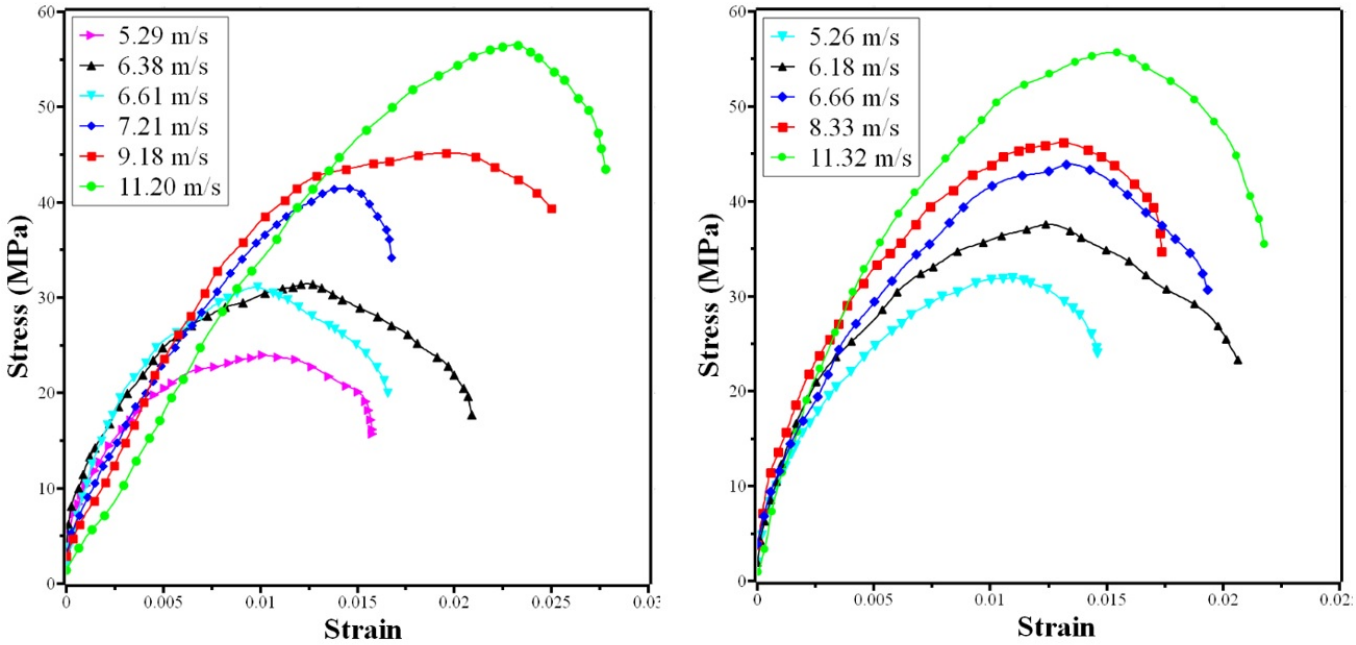

(a) C-G complex (b) G-C complex

Figure 9: Dynamic stress-strain curve of layered composite coal-rock

3.1.2.2 The impact of impact speed on dynamic performance

Figure 10 is a graph showing the relationship change between the impact velocity and the peak stress of the layered composite coal-rock. It can be clearly seen from the Figure that as the impact velocity continues to increase, the peak stress increases linearly, and the peak stress of the G-C composite is always greater than that of the C-G composite, and this trend gradually decreases as the speed increases. When the stress wave propagates backward from the incident rock mass, reflection and transmission will occur at the junction of the two rock masses. Taking the G-C composite rock mass as an example, the relationship model of the incident wave, reflected wave and transmitted wave is shown in Figure 11. According to the assumption of uniform stress, continuous boundary conditions and Newton's third law, after stress wave reflection and transmission, the particles on both sides of the interface between white sandstone and coal should be the same regardless of velocity or stress. From the conservation of wave front momentum, it can be seen that the dynamic load stress of the coal cell caused by the transmitted stress wave σ_{Td} and the dynamic load stress σ_{Rd} of the white sandstone caused by the reflected stress wave are:

$$\sigma_{Td} = \frac{2}{1+n}\sigma_{Id} \tag{9}$$

$$\sigma_{Rd} = \frac{1-n}{1+n}\sigma_{Id} \tag{10}$$

$$n = \frac{\rho_G C_G}{\rho_C C_C} \tag{11}$$

In the formula, σ_{Id} is the incident wave amplitude stress;ρ_G,C_G are the density of the white sandstone and the elastic longitudinal wave velocity, respectively; ρ_C, C_C are the density of the coal monomer and the elastic longitudinal wave velocity, n is the white sandstone The ratio of the wave impedance of sandstone and coal alone.

Bringing into the wave impedance of white sandstone and coal monomer respectively, it can be found that the absolute value of the dynamic load stress of white sandstone σ_{Rd} is always smaller than the dynamic load stress of coal monomer σ_{Td}, andwith the continuous increase of incident wave amplitude stress, this kind of influence is constantly increasing.Compared with the GC complex and the CG complex, the GC complex has a better impedance matching effect, so it will produce smaller reflected waves, and more waves will pass through the sample into the transmission rod, but as the incident wave continues to increase , The effect of wave impedance matching on the propagation of stress waves gradually weakens. Similar to the phenomenon observed in Fig. 10, it can be explained that the G-C composite has a better impedance matching effect than the C-G composite and the incident rod, and the energy transfer effect is better.

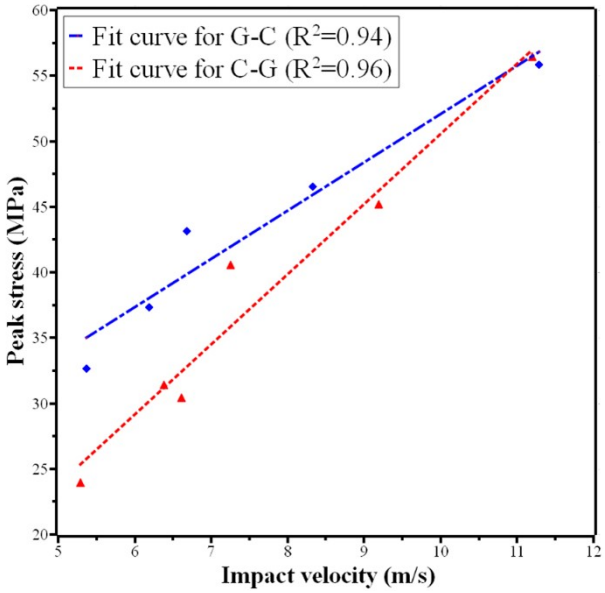

Figure 10: The relationship between impact velocity and peak stress

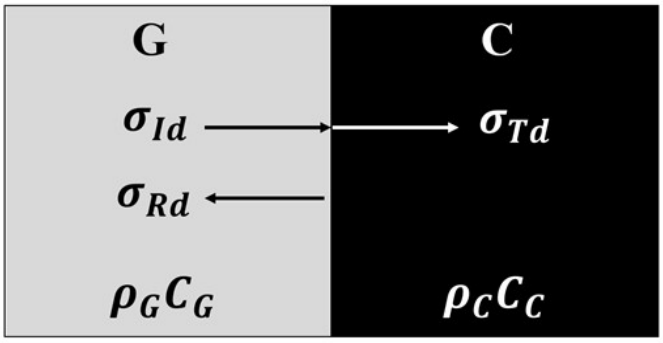

Figure 11: The transmission and reflection relationship model of the stress wave at the coal-rock junction

The relationship between impact velocity and DIF (Dynamic Increase Factor) is shown in Figure 12. DIF is a commonly used concept in the concrete field, used to measure the strength of the dynamic performance of concrete. This concept is introduced here to measure the performance difference of coal-rock composites under dynamic load and static load. It can be seen from the Figure 12 that DIF increases linearly with the increase of the impact speed, and this trend gradually weakens with the increase of the speed. This is because when the white sandstone is close to the incident rod, the wave impedance matching effect is better, so better dynamic performance can be obtained. When the incident speed is low, the wave impedance matching effect has a greater impact on the dynamic performance. The better the matching effect, the better the energy transfer effect. At higher impact speeds, the incident stress wave begins to increase, and the effect of wave impedance matching gradually weakens, resulting in similar dynamic performance of the two types of layered composite rock masses.

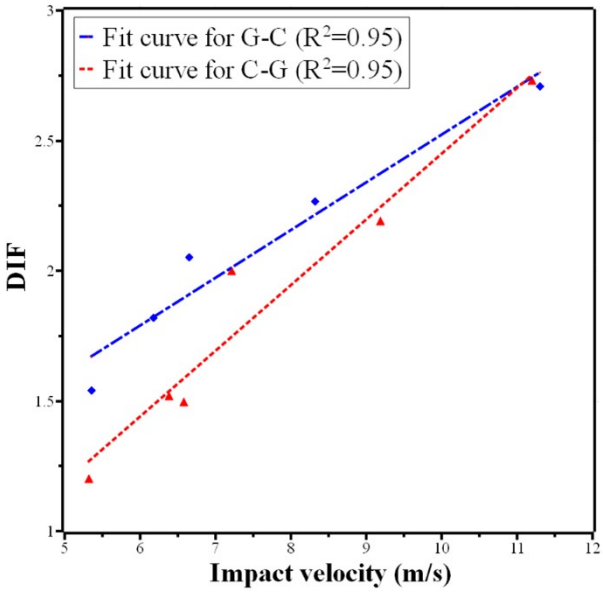

Figure 12: The relationship between impact velocity and DIF

3.2 Energy dissipation analysis

In the process of rock mass fracture, energy transformation runs through it. Material destruction is essentially a process of gradual imbalance of the state driven by energy. Energy dissipation,like in Fengnian (2004), Zhao (2008), Liu (2016) and Xie (2008) is also the main cause of rock damage and deformation. During the SHPB experiment, according to the one-dimensional elastic wave theory, the energy carried by the stress wave is:

$$W_I = \frac{C_e A_e}{E_e} \int \sigma_I^2(t) dt \tag{12}$$

$$W_R = \frac{C_e A_e}{E_e} \int \sigma_R^2(t) dt \tag{13}$$

$$W_T = \frac{C_e A_e}{E_e} \int \sigma_T^2(t) dt \tag{14}$$

In the formula, W_I, W_R, W_T are the incident wave, reflected wave, and transmitted wave energy respectively; A_e and $E_e$are the elastic modulus and cross-sectional area of the pressure rod; C_e is the propagation velocity of the stress wave in the pressure rod;$\sigma_I(t), \sigma_R(t), \sigma_T(t)$ are the incident, reflection, and transmission stress at time t, respectively.

Without considering the loss, the energy absorbed by the layered composite rock mass during the crushing process, that is, the dissipated energy W_S is:

$$W_S = W_I - W_T - W_R \tag{15}$$

Comparing the dissipated energy density $\omega_d$of the rock per unit volume can better characterize the amount of energy absorbed by rock fragmentation. The dissipated energy density $\omega_d$is:

$$\omega_d = \frac{W_S}{V} \tag{16}$$

In the formula, V is the volume of the layered composite.

Similarly, the incident energy density ω_I can be obtained as:

$$\omega_d = \frac{W_I}{V} \tag{17}$$

Figure 13 shows the relationship between impact velocity and incident energy.It can be found that the incident energy has nothing to do with the sample, only the impact velocity. Whether it is a G-C composite or a C-G composite, the incident energy increases linearly with the increase of the impact velocity.

Figure 14 is a graph of the relationship between incident energy density and dissipated energy density. Affected by the wave impedance matching relationship, the dissipated energy density increases with the increase of the incident energy density in a quadratic function. With the continuous increase of incident energy, the influence of wave impedance matching on the density of dissipated energy is gradually decreasing. Therefore, more incident energy will result in higher dissipated energy, and the rock will be broken more fully. From the relationship between the impact velocity and incident energy in Figure 13, it can be seen that the incident energy is basically the same at the same velocity, so the GC complex absorbs more energy for its own crack incubation and expansion, and also has a higher energy utilization rate.

We can find that under the same incident energy, the better the wave impedance matching effect of the rock, the more energy will be dissipated, and the rock will absorb more energy for its own crushing, the crushing effect is better, and the energy utilization rate is higher. This situation has also been verified and applied in the field of blasting [26].

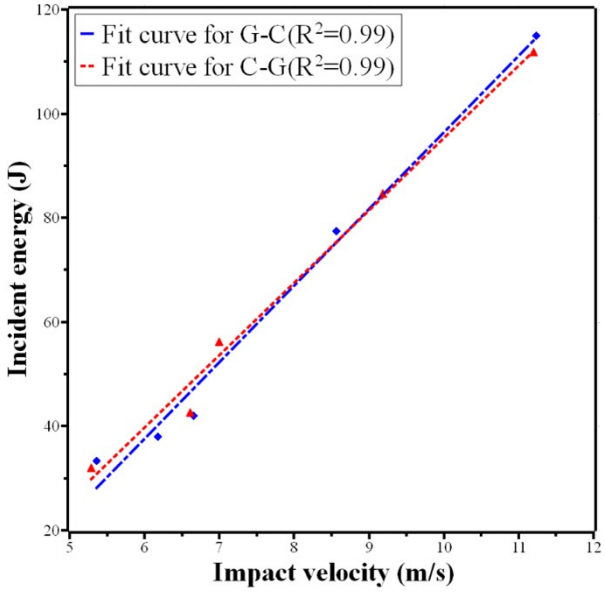

Figure 13: The relationship between impact velocity and incident energy

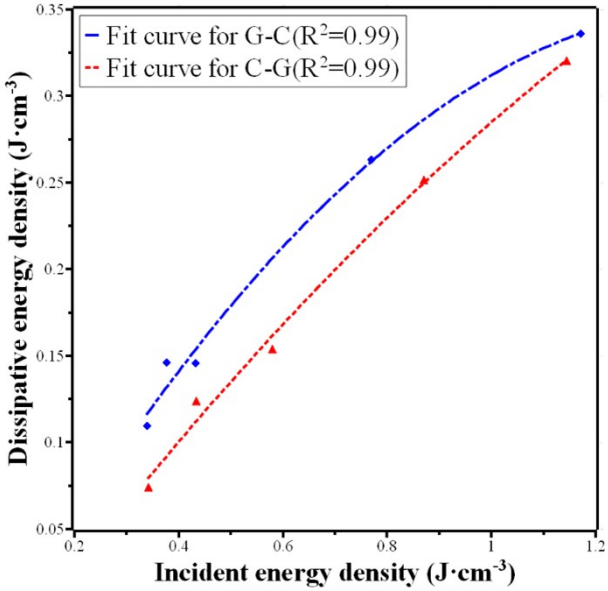

Figure 14: The relationship between incident energy density and dissipated energy density

3.3 Fractal characteristics of impact damage

The fractal dimension can quantitatively and intuitively reflect the degree of fracture of a rock sample. Generally speaking, the higher the fractal dimension, the greater the degree of fracture, like in Liu et al. (2020), Lee et al. (1990) and Hirata (1989). layered composite coal-rock is a combination of single coal and roof rock. In the process of geotechnical construction, the explosion work of complexes of different lithologies is often encountered. The fractal characteristics of its failure are studied, and the underground stress disturbance and blasting Such optimization is of great significance.

In order to quantitatively describe the damage distribution of the layered composite coal-rock under dynamic load, this paper uses the equivalent side length-particle size distribution to calculate the fractal dimension, like in Turk et al. (1987), the formula is as follows:

$$D = 3 - \alpha \tag{18}$$

$$\alpha = \frac{lg(M_r/M_t)}{lg\, L_r} \tag{19}$$

In the formula, D is the fractal dimension of the sample, α is the slope value of M_r/M_t-L_r in double logarithmic coordinates,$L_r$is the equivalent particle size of the damage, and $M_r$is the equivalent particle size <L_r of the damage Cumulative mass,$M_t$is the total mass of damaged objects in the calculation scale.

Taking into account the quality requirements of particle size analysis of damaged materials, this test uses screens with particle sizes of 1.25mm, 2.5mm, 5mm, 10mm, 15mm, 20mm, 25mm, and 30mm to screen the damaged samples. The length, width and thickness of the damaged objects larger than 30mm are manually measured and weighed. The fractal calculation results of the damaged objects after the sample is broken are shown in Table 4.

Table 4 Fractal statistics of particle size of damaged material of layered composite coal-rock

Sample number	Impact velocity v(m/s)	Cumulative mass of damaged material with different particle size M_r(g)											Total mass M_t(g)	D
		<1.25 mm	1.25 mm	2.5 mm	5 mm	10 mm	15 mm	20 mm	25 mm	30 mm	40 mm	50 mm		
CG-1	5.29	1	1	2	1	2	6	0	0	22	151	0	195	1.90
CG-2	6.38	4	3	11	16	10	3	3	0	44	90	0	181	2.09
CG-3	6.61	3	4	8	14	2	4	0	0	17	127	0	179	2.14
CG-4	7.21	9	7	13	14	5	3	44	14	79	0	0	191	2.20
CG-5	9.19	15	9	20	17	14	0	39	0	83	0	0	184	2.32
CG-6	11.20	20	10	16	19	18	18	46	20	22	0	0	198	2.36
GC-1	5.36	2	2	6	11	14	3	0	0	24	126	0	187	1.94
GC-2	6.18	5	4	7	10	7	10	0	0	142	0	0	183	2.11
GC-3	6.66	8	5	12	14	2	11	26	0	108	0	0	188	2.18
GC-4	8.33	13	9	19	19	2	0	26	18	85	0	0	193	2.32
GC-5	11.32	15	9	11	16	10	3	3	0	44	90	0	188	2.36

Figure 15 shows the relationship between the impact velocity and the fractal dimension. It can be found that with the continuous increase of the impact velocity, the fractal dimension of the layered composite coal-rock also keeps increasing, showing a positive correlation. It shows that the greater the impact velocity, the greater the fractal dimension of the sample after fragmentation, the smaller the particle size of the damaged material, and the greater the degree of damage. But as the impact speed continues to increase, this trend is gradually slowing down. At the same speed, the fractal dimension of the GC complex is greater than the fractal dimension of the CG complex. This is because under the same conditions, the wave impedance of the GC complex and the wave impedance of the pressure rod are more matched, and the energy transfer effect is better. So the degree of fragmentation is also higher. However, as the speed increases, the fractal dimensions of the two layered composite coal-rocks are gradually approaching. This is because the overall fracture of the layered composite coal-rock is often caused by the release of elastic energy due to the collapse of coal components. Resulting in broken assembly. When the speed increases to a certain extent, the threshold value of

the storage elastic energy of the coal component has nothing to do with the transmission direction, so the degree of fragmentation also begins to approach.

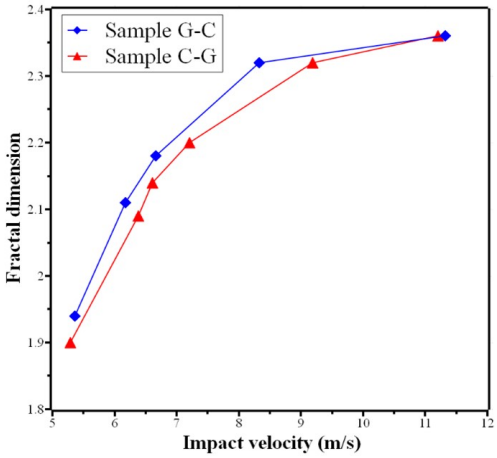

Figure 15: The relationship between impact velocity and fractal dimension

3.4 Impact failure mode

3.4.1 Meso-damage mode

Figure 16 is the SEM scanning image of each part of the layered composite coal-rock after it is broken. The damage of the sample is mainly due to the generation and expansion of cracks. Compared with white sandstone, the internal structure of coal alone determines that it is easier to produce and converge cracks until it is destroyed, while white sandstone is denser and less prone to cracks. Therefore, as shown in Figure (a), (b), and (c), there are many and miscellaneous fissures produced by the single coal. Under the action of external pressure, the small internal fissures continue to expand and extend, eventually leading to the destruction of the entire rock. The white sandstone has a small number of fissures, but it is easy to produce a split surface that penetrates the rock sample, which eventually leads to rock failure. For the layered composite coal-rock, when one of the rocks is broken, its cracks will also extend to the other rock, eventually causing overall destruction. As shown in Figure (d), the presence of impurities in the coal alone will also make it easier for the rock itself to produce cracks along the interface, and generally speaking, such cracks are relatively regular.

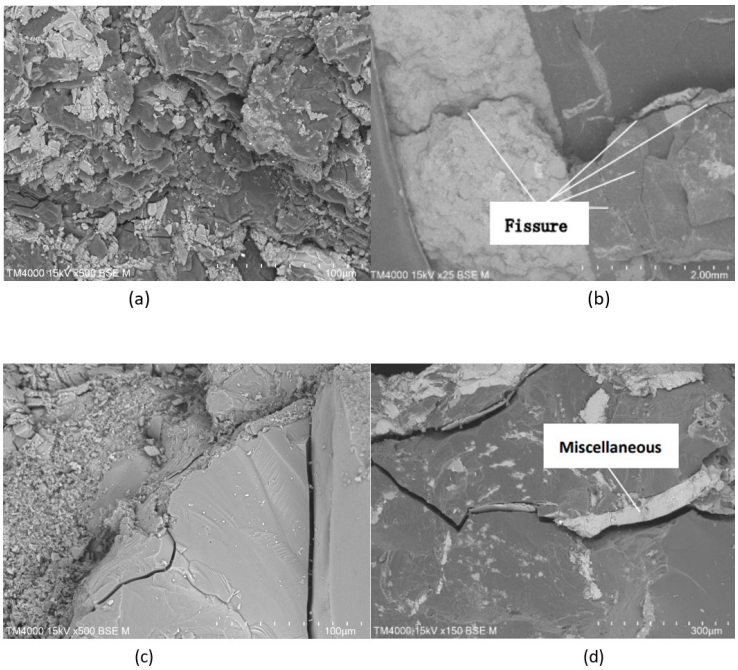

Figure 16: SEM scanning image of layered composite coal-rock. (a) SEM scanning image of single coal; (b) SEM scanning image of the junction of layered composite coal-rock; (c) SEM scan of white sandstone; (d) SEM scan of internal fissures of coal monomer

3.4.2 Macroscopic damage pattern

Figure 17 is the failure form of the layered composite coal-rock after pressurization by the computer-controlled electro-hydraulic servo rock pressure testing machine. It can be found that under the action of static impact, whether it is the CG composite or the GC composite coal component is broken the degree is greater than that of the white sandstone component. There are many small cracks in the coal component, which are more likely to gather and grow, causing the coal component to collapse as a whole. The white sandstone component has higher internal density and fewer internal defects, so the fractures transferred from the coal component will continue to derive along the coal-rock interface, resulting in a split surface that penetrates the white sandstone. Under the action of the compaction stage of the CG complex, the macroscopic characterization of the coal component with more internal defects will change greatly. Under the action of the compaction stage of the CG complex, the macroscopic characterization of the coal component with more internal defects will change greatly. The coal component will extend to the periphery to form a truncated cone shape, and this extension phenomenon will also accelerate the splitting of the white sandstone component. The macroscopic characterization of the G-C complex has not changed much.

Figure 18 and 19 show the impact failure modes of two layered coal-rock assemblies in SHPB under different impact speeds. According to the conclusion in section 3.3, the greater the impact velocity, the more severe the damage of the sample and the smaller the particle size of the damaged material. In the Figure, the failure morphology of the two layered composite coal-rocks is similar, but the particle size of the damaged material of the G-C composite is slightly smaller than that of the C-G composite at the same speed. The damage degree of the coal component in the layered composite coal-rock is often more severe than that of the white sandstone component. In the experiment, it is found that the equivalent particle size of the white sandstone component is mostly larger than 15mm, while the equivalent particle size of the coal rock component is mostly less than 10mm, which is determined by the internal structure of different components. A large number of internal defects in the coal and rock composition cause the internal cracks to be more likely to incubate and derive under the action of external loads, which leads to the overall crushing of the sample. Observing the changes in the fracture morphology of the coal component, it can be found that the coal component exhibits shear failure at low speeds. With the increase of the speed, the split surface gradually appears. Under the combined action of shear and splitting, the coal component The minute is gradually crushed into fine particles. As the speed increases, the white sandstone component increases shear failure, resulting in the continuous decrease of the particle size of the white sandstone component. Compared with the broken shape under static impact, the white sandstone under dynamic impact is more likely to produce a split surface that penetrates the sample and cause damage, and the coal rock is also more likely to fragment into smaller-sized damage.

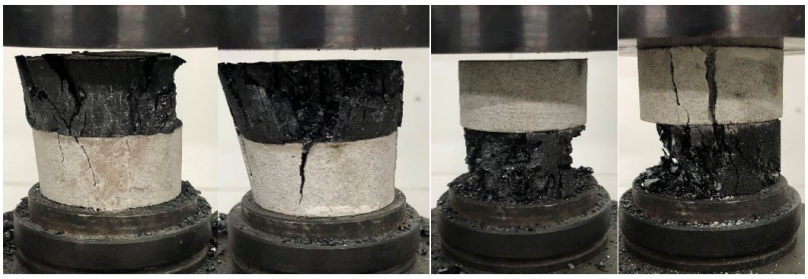

(a) C-G complex (b) G-C complex

Figure 17: Uniaxial compression failure mode of layered composite coal-rock

(a) 5.29 m/s (b) 6.61 m/s (c) 9.19 m/s (d) 11.2 m/s

Figure 18: C-G composite body dynamic impact damage morphology

(a) 5.36 m/s (b) 6.18 m/s (c) 8.33 m/s (d) 11.32 m/s

Figure 19: G-C composite body dynamic impact damage morphology

4 CONCLUSION

Using the separated Hopkinson pressure bar testing device (SHPB) and the microcomputer-controlled electro-hydraulic servo rock pressure testing machine experimental system, a series of related studies on the mechanical properties of the layered composite coal-rock were carried out, and the following conclusions were obtained:

1. Under static load, the strength of the layered composite coal-rock will be slightly higher than that of a single rock body. The change of the impact direction will not affect the strength of the composite, but the rupture time course of the C-G composite body will be shorter than the rupture time course of the G-C composite body.
2. The layered composite coal-rock is under the action of dynamic load, as the impact velocity increases, the intensity and DIF gradually increase. Because the impedance matching effect between the G-C complex and the strut is better, the peak stress of the G-C complex is always greater than that of the C-G complex, and this trend gradually decreases with increasing speed. In the same way, DIF also changes in this pattern.
3. During the loading process of the layered composite coal-rock, the dissipated energy density increases with the increase of the incident energy density in a quadratic function. When the speed is the same, affected by the matching effect of wave impedance, when the stress wave changes from hard to soft, the dissipated energy density is greater thanfrom soft to hard, and more energy will be absorbed for self-breaking. However, as the impact speed gradually increased, the difference between the two gradually decreased.
4. The fractal dimension of the layered composite coal-rock after it is broken under dynamic load increases with the increase of speed, which shows that the damage of the composite body is related to the impact velocity, but this connection will be affected by wave impedance matching. The effect of the effect is that at the same impact velocity, the GC complex with better impedance matching has a larger fractal dimension.
5. Under the action of static load, the layered composite coal-rock is not broken to a high degree, and it is easy to produce a macroscopic cleavage surface penetrating the composite body. Under the action of dynamic load, the degree of fragmentation of the coal component is much greater than that of the white sandstone component. The white sandstone component is mostly sheared and the coal component is mostly crushed. With the increase of impact speed, this trend becomes more and more obvious.

Acknowledgements

The work was finacially supported by the Special Fund Project for Fundamental Scientific Research Expenses of Central Universities (Grant No. FRF-IDRY-20-024) and National Natural Science Foundation of China (Grant No. 51504016).

Author Contributions: Conceptualization, Shizhuo Zou and Yu Zhou; Investigation, Shizhuo Zou and Li Wang; Methodology, Shizhuo Zou and Xiaoling Wu; Resources, Shizhuo Zou and Jianmin Wen; Supervision, Shizhuo Zou and Yu Zhou; Validation, Shizhuo Zou and Yu Zhou; Writing – original draft, Shizhuo Zou, Li Wang, Jianmin Wen, Xiaoling Wu and Yu Zhou; Writing – review & editing – Preparation, Shizhuo Zou and Yu Zhou.

Editor: Marcílio Alves.

References

Dou, L. M., Lu, C. P., Mu, Z. L., Zhang, X. T., & Li, Z. H. (2006). Rock burst tendency of coal-rock combinations sample. Journal of Mining & Safety Engineering, 23(1), 43-46.

Zhao, Y. X., Jiang, Y. D., Zhu, J., & Sun, G. Z. (2008). Experimental study on precursory information of deformations of coal-rock composite samples before failure. Chin J Rock Mech Eng, 27(2), 339-346.

Shan, P., & Lai, X. (2020). An associated evaluation methodology of initial stress level of coal-rock masses in steeply inclined coal seams, Urumchi coal field, China. Engineering Computations.

Wang, H., Jiang, C., Zheng, P., Zhao, W., & Li, N. (2020). A combined supporting system based on filled-wall method for semi coal-rock roadways with large deformations. Tunnelling and Underground Space Technology, 99, 103382.

Shen, B. (2014). Coal mine roadway stability in soft rock: a case study. Rock Mechanics and Rock Engineering, 47(6), 2225-2238.

Liu, X. S., Tan, Y. L., Ning, J. G., Lu, Y. W., & Gu, Q. H. (2018a). Mechanical properties and damage constitutive model of coal in coal-rock combined body. International Journal of Rock Mechanics and Mining Sciences, 110, 140-150.

Li, Y., Zhang, S., & Zhang, X. (2018b). Classification and fractal characteristics of coal rock fragments under uniaxial cyclic loading conditions. Arabian Journal of Geosciences, 11(9), 1-12.

Wen, Z., Wang, X., Chen, L., Lin, G., & Zhang, H. (2017). Size effect on acoustic emission characteristics of coal-rock damage evolution. Advances in Materials Science and Engineering, 2017.

Huang, B. X., Cheng, Q. Y., Liu, C. Y., Wei, M. T., & Fu, J. H. (2011). Hydraulic fracturing theory of coal-rock mass and its technical framework. J. Min. Saf. Eng, 28(2), 167-173.

Guo, D. M., Zuo, J. P., Zhang, Y., & Yang, R. S. (2011). Research on strength and failure mechanism of deep coal-rock combination bodies of different inclined angles. Rock and Soil Mechanics, 32(5), 1333-1339.

Zuo, J. P., Xie, H. P., Wu, A. M., & Liu, J. F. (2011). Investigation on failure mechanisms and mechanical behaviors of deep coal-rock single body and combined body. Chinese Journal of Rock Mechanics and Engineering, 30(1), 84-92.

Li, X., Chen, S., Wang, E., & Li, Z. (2021). Rockburst mechanism in coal rock with structural surface and the microseismic (MS) and electromagnetic radiation (EMR) response. Engineering Failure Analysis, 124, 105396.

Song, D., Wang, E., & Liu, J. (2012). Relationship between EMR and dissipated energy of coal rock mass during cyclic loading process. Safety Science, 50(4), 751-760.

Yin, T. B., Peng, K., Wang, L., Wang, P., Yin, X. Y., & Zhang, Y. L. (2016). Study on impact damage and energy dissipation of coal rock exposed to high temperatures. Shock and Vibration, 2016.

Chen, S. (2018). Numerical simulation of split-hopkinson pressure bar test on high-density polyethylene. Chemical Engineering Transactions, 66, 271-276.

Gong, F., Ye, H., & Luo, Y. (2018). The effect of high loading rate on the behaviour and mechanical properties of coal-rock combined body. Shock and vibration, 2018.

Li, D., Han, Z., Zhu, Q., Zhang, Y., & Ranjith, P. G. (2019). Stress wave propagation and dynamic behavior of red sandstone with single bonded planar joint at various angles. International Journal of Rock Mechanics and Mining Sciences, 117, 162-170.

Zhao, X., Xu, S., Li, Q., & Chen, B. (2019). Coupled effects of high temperature and strain rate on compressive properties of hybrid fiber UHTCC. Materials and Structures, 52(5), 1-17.

Zhu, J., Hu, S., & Wang, L. (2009). An analysis of stress uniformity for concrete-like specimens during SHPB tests. International Journal of Impact Engineering, 36(1), 61-72.

Malvar, L. J., & Crawford, J. E. (1998). Dynamic increase factors for concrete.

Feng, S., Zhou, Y., Wang, Y., & Lei, M. (2020). Experimental research on the dynamic mechanical properties and damage characteristics of lightweight foamed concrete under impact loading. International Journal of Impact Engineering, 140, 103558.

Comité Euro-International du Béton. (1993). CEB-FIP model code 1990: Design code. Thomas Telford Publishing.

Fengnian, J., Meirong, J., &Xiaoling, G. (2004). Defining damage variable based on energy dissipation. Chinese Journal of Rock Mechanics and Engineering, 23(12), 1976-1980.

Zhao, Z. H., &Xie, H. P. (2008). Energy transfer and energy dissipation in rock deformation and fracture. JOURNAL-SICHUAN UNIVERSITY ENGINEERING SCIENCE EDITION, 40(2), 26.

Liu, X. S., Ning, J. G., Tan, Y. L., & Gu, Q. H. (2016). Damage constitutive model based on energy dissipation for intact rock subjected to cyclic loading. International journal of rock mechanics and mining sciences, 85, 27-32.

Xie, H. P., Ju, Y., Li, L. Y., & Peng, R. D. (2008). Energy mechanism of deformation and failure of rock masses. Chinese Journal of Rock Mechanics and Engineering, 27(9), 1729-1740.

Liu, R., Zhu, Z., Li, Y., Liu, B., Wan, D., & Li, M. (2020). Study of rock dynamic fracture toughness and crack propagation parameters of four brittle materials under blasting. Engineering Fracture Mechanics, 225, 106460.

Lee, Y. H., Carr, J. R., Barr, D. J., & Haas, C. J. (1990, December). The fractal dimension as a measure of the roughness of rock discontinuity profiles. In International journal of rock mechanics and mining sciences & geomechanics abstracts (Vol. 27, No. 6, pp. 453-464). Pergamon.

Hirata, T. (1989). Fractal dimension of fault systems in Japan: Fractal structure in rock fracture geometry at various scales. In Fractals in geophysics (pp. 157-170). Birkhäuser, Basel.

Turk, N., Greig, M. J., Dearman, W. R., & Amin, F. F. (1987, June). Characterization of rock joint surfaces by fractal dimension. In The 28th US symposium on rock mechanics (USRMS). OnePetro.